Fermi Surface Topology and the Upper Critical Field in Two-Band Superconductors: Application to MgB_2

T. Dahm and N. Schopohl

Institut für Theoretische Physik, Universität Tübingen, Auf der Morgenstelle 14, D-72076 Tübingen, Germany

(Received 9 December 2002; published 1 July 2003)

Recent measurements of the anisotropy of the upper critical field B_{c2} on MgB_2 single crystals have shown a puzzling strong temperature dependence. Here, we present a calculation of the upper critical field based on a detailed modeling of band structure calculations that takes into account both the unusual Fermi surface topology and the two gap nature of the superconducting order parameter. Our results show that the strong temperature dependence of the B_{c2} anisotropy can be understood as an interplay of the dominating gap on the σ band, which possesses a small c-axis component of the Fermi velocity, with the induced superconductivity on the π-band possessing a large c-axis component of the Fermi velocity. We provide analytic formulas for the anisotropy ratio at $T = 0$ and $T = T_c$ and quantitatively predict the distortion of the vortex lattice based on our calculations.

DOI: 10.1103/PhysRevLett.91.017001 PACS numbers: 74.20.–z, 71.18.+y, 74.25.Op, 74.70.Ad

Our understanding of the physical properties of the recently discovered superconductivity in MgB_2 has made rapid progress since its discovery [1]. Its high critical temperature $T_c = 39$ K can be understood from strong conventional electron-phonon coupling to a high frequency phonon mode [2–4]. Its pairing symmetry seems to be of conventional s-wave type [5,6]. However, in contrast to conventional superconductors, a number of recent experiments indicate that there exist two gaps of different size in this compound [7–12]. This possibility is supported by band structure calculations, which have shown that the Fermi surface of this compound consists of four bands: two σ-type two-dimensional cylindrical hole sheets and two π-type three-dimensional tubular networks [13,14] in good agreement with recent de Haas–van Alphen experiments [15]. Microscopic calculations of the superconducting gap based on band structure calculations have shown that indeed one should expect a big superconducting gap living on the σ bands and a smaller one, induced by interband pairing interaction, living on the π bands [3,16]. Impurity scattering, which tends to average out strongly differing gap values, in this case becomes ineffective, because the σ and π bands possess different symmetries, making interband impurity scattering much weaker than intraband impurity scattering [17]. Recent measurements of the upper critical field B_{c2}, particularly its anisotropy, on single crystal MgB_2 have shown a puzzling strong temperature dependence of the anisotropy ratio B_{c2}^{ab}/B_{c2}^{c} between the ab plane and the c-axis upper critical field [18–20]. In conventional systems this ratio rarely changes by more than 10%–20% as a function of temperature. In MgB_2 changes by more than a factor of 2 have been observed. It has been shown that such a strong temperature dependence of the anisotropy ratio can be obtained within a strongly anisotropic single gap model, possessing a small gap in c-axis direction and a big gap in ab-plane direction [21]. However, the gap anisotropy would have to be a factor of 10, which is too big as compared with experimental values. In addition, this scenario would be inconsistent with penetration depth studies which clearly indicate the presence of a small gap within the ab plane [22,23].

Here, we present first calculations of the upper critical field B_{c2}, which take into account the multiband Fermi surface structure seriously. We show that the strong temperature dependence of the anisotropy of B_{c2} can be traced back to the influence of the two topologically very different Fermi surfaces. While the cylindrical Fermi surface sheets are dominating the behavior of B_{c2} at low temperatures, leading to a large anisotropy, at temperatures approaching T_c the π bands due to their much larger c-axis Fermi velocity play a more important role, strongly reducing the anisotropy. Thus, the strong temperature dependence of the B_{c2} anisotropy appears as a crossover from a low temperature σ band dominated regime to a higher temperature mixed σ and π band regime.

In order to include the multiband Fermi surface structure in the calculation of the upper critical field, we start our investigation from the fully momentum dependent multiband formulation of the quasiclassical (Eilenberger) theory of the upper critical field [24]. For that purpose we have to solve the linearized multiband gap equation in the presence of an external magnetic field, which reads

$$\Delta_\alpha(\vec{r}) = -\pi T \sum_{\alpha'} \sum_{|\omega_n'|<\omega_c} \lambda^{\alpha\alpha'} \langle f_{\alpha'}(\vec{r}, \hat{k}'; \omega_n') \rangle_{\alpha'}. \quad (1)$$

Here, f_α is the anomalous Eilenberger propagator on the Fermi surface sheet denoted by α. Δ_α is the gap function on that Fermi surface sheet and $\lambda^{\alpha\alpha'}$ is the pairing interaction, which becomes a matrix in the band

indices. The brackets $\langle \cdots \rangle_{\alpha'}$ denote a Fermi surface average over momentum $\hat{k}'$ of the Fermi surface sheet α'. In Eq. (1) we have already assumed that the gaps are isotropic s wave on the Fermi surfaces, as indicated by experiment, but may have different values on different sheets. At B_{c2} the anomalous Eilenberger propagator has to be determined from the linearized Eilenberger equation (for $\omega_n > 0$)

$$\left\{\omega_n + \vec{v}_{F,\alpha}\left[\frac{\hbar}{2}\vec{\nabla} - i\frac{e}{c}\vec{A}(\vec{r})\right]\right\} f_\alpha(\vec{r}, \hat{k}; \omega_n) = -\Delta_\alpha(\vec{r}). \tag{2}$$

Here, $\vec{v}_{F,\alpha}$ is the (momentum dependent) Fermi velocity on Fermi surface sheet α and $\vec{A}$ the vector potential due to the magnetic field $\vec{B} = \vec{\nabla} \times \vec{A}$. Equations (1) and (2) constitute an eigenvalue problem for $\Delta_\alpha(\vec{r})$. For a given temperature T the solution $\Delta_\alpha(\vec{r})$ which solves Eqs. (1) and (2) for the highest value of B determines B_{c2}.

Usually this eigenvalue problem is solved by a Landau level expansion of $\Delta_\alpha(\vec{r})$ above the Abrikosov ground state of the vortex lattice. It has been shown recently, however, that a variational ansatz for $\Delta_\alpha(\vec{r})$ corresponding to a *distorted* Abrikosov lattice leads to much better results for strongly anisotropic systems [21], and we will adopt that method here. In this method the ansatz reads $\Delta_\alpha(\vec{r}) = \Delta_\alpha \psi_\Lambda^\tau(\vec{r})$ with $\psi_\Lambda^\tau(x, y) = \psi_\Lambda(e^{-\tau}x, e^{\tau}y)$. Here, ψ_Λ is the usual Abrikosov ground state and τ is a variational parameter describing the distortion of the vortex lattice. The undistorted lattice corresponds to $\tau = 0$ and τ has to be determined by maximizing B_{c2}. Introducing this ansatz into Eqs. (1) and (2) and using standard operator techniques (see, e.g., Refs. [24–27]) we are led to the following eigenvalue problem for Δ_α in band space:

$$\Delta_\alpha = \sum_{\alpha'} \lambda^{\alpha\alpha'}\left[\frac{1}{\lambda_+} - \ln\frac{T}{T_c} - l_{\alpha'}\left(\tau, \frac{B_{c2}}{T^2}\right)\right]\Delta_{\alpha'}. \tag{3}$$

Here, λ_+ is the highest eigenvalue of $\lambda^{\alpha\alpha'}$, which determines T_c. The function l_α is given by the expression

$$l_\alpha = \int_0^\infty \frac{du}{\sinh u}\langle 1 - e^{-u^2(eB_{c2}/8\pi^2T^2)[e^{-2\tau}v_{F1,\alpha}^2(\hat{k}) + e^{2\tau}v_{F2,\alpha}^2(\hat{k})]}\rangle_\alpha. \tag{4}$$

Here, $v_{F1,\alpha}$ and $v_{F2,\alpha}$ are the components of the Fermi velocity perpendicular to the magnetic field $\vec{B}$ on Fermi surface α. According to Eq. (3) the criterion for B_{c2} is that the highest eigenvalue of the matrix $\lambda^{\alpha\alpha'}[\frac{1}{\lambda_+} - \ln\frac{T}{T_c} - l_{\alpha'}(\tau, \frac{B_{c2}}{T^2})]$ becomes 1. Apparently, at $T = T_c$ this is fulfilled for $B_{c2} = 0$, because $l_\alpha \to 0$.

Equations (3) and (4) allow one to determine the temperature dependence and angular dependence of B_{c2} from microscopic grounds. The material parameters we need for the solution are the Fermi velocities $\vec{v}_{F,\alpha}(\hat{k})$ and the coupling matrix $\lambda^{\alpha\alpha'}$, which can be taken from band structure calculations. In order to simplify the analysis we restrict ourselves to two relevant bands, because the two σ bands and the two π bands are very similar [3]. The σ band can be described to a good approximation by a cylindrical Fermi surface with a small c-axis hopping parameter. The π band can be modeled by a half-torus as shown in Fig. 1 (for comparison see the Γ-point centered Fermi surfaces in Ref. [13]). Fermi velocities are thus $\vec{v}_{F,\pi}(\theta, \phi) = v_{F\pi}(\cos\theta\cos\phi, \cos\theta\sin\phi, \sin\theta)$ and $\vec{v}_{F,\sigma}(k_c, \phi) = v_{F\sigma}(\cos\phi, \sin\phi, \epsilon_c \sin ck_c)$. Here, ϕ is the azimuthal angle within the ab plane, $\theta \in [\frac{\pi}{2}, \frac{3\pi}{2}]$ the polar angle of the torus, k_c the c-axis component of the momentum, and c the lattice constant in the c direction. The dimensionless parameter ϵ_c describes the small c-axis dispersion of the cylinder. The Fermi surface averages over the cylinder and the torus are then given by $\langle \cdots \rangle_\sigma = \frac{c}{4\pi^2}\int_{-\pi/c}^{\pi/c} dk_c \int_0^{2\pi} d\phi \cdots$ and $\langle \cdots \rangle_\pi = \frac{1}{2\pi^2}\int_{\pi/2}^{3\pi/2} d\theta \int_0^{2\pi} d\phi \frac{1+\kappa\cos\theta}{1-2\kappa/\pi}\cdots$, where κ is the ratio of the two radii of the torus. The parameters of the Fermi velocities can be found from band structure calculations. Taking the values given in Ref. [28], we determine $v_{F\pi} = 8.2 \times 10^5$ m/s, $v_{F\sigma} = 4.4 \times 10^5$ m/s, and $\epsilon_c = 0.23$. The ratio of the two radii of the torus can be estimated from the Fermi surface crossings in Ref. [14] to be about $\kappa = 0.25$.

For a 2×2 matrix $\lambda^{\alpha\alpha'}$ the criterion that the biggest eigenvalue of Eq. (3) becomes 1 leads to the equation $(1 - \eta)l_\sigma + \eta l_\pi + \ln t = -\Lambda_\pm(l_\sigma + \ln t)(l_\pi + \ln t)$. Here, $t = T/T_c$, λ_- is the smaller eigenvalue of $\lambda^{\alpha\alpha'}$, and $\eta = \frac{\lambda^{\pi\pi} - \lambda_-}{\lambda_+ - \lambda_-}$ is a dimensionless parameter describing the interband coupling strength of the two bands ($\eta = 0$ corresponds to no coupling, $\eta = 0.5$ to maximum coupling). From band structure calculations in Ref. [3] the following effective matrix elements can be obtained: $\lambda^{\sigma\sigma} = 0.959$, $\lambda^{\sigma\pi} = 0.222$, $\lambda^{\pi\sigma} = 0.163$, and $\lambda^{\pi\pi} = 0.278$. From these we find $\lambda_+ = 1.008$, $\lambda_- = 0.228$, and $\eta = 0.064$. As it

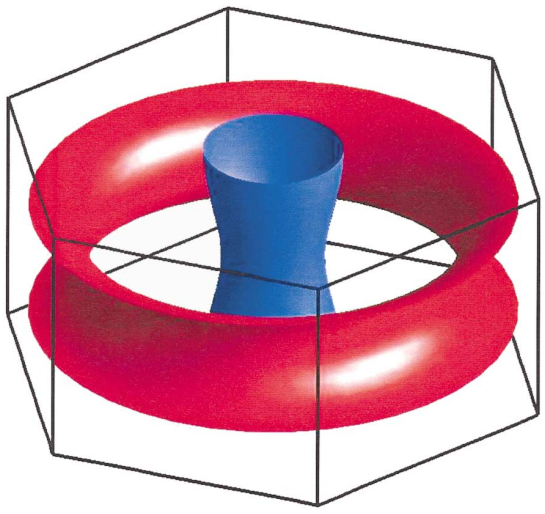

FIG. 1 (color). Fermi surface topology used for the calculation of B_{c2} in this work. The π band is modeled by a half-torus, the σ band by a distorted cylinder.

turns out the remaining parameter $\Lambda_{\pm} = \frac{\lambda_+\lambda_-}{\lambda_+ - \lambda_-}$ only weakly affects the results as soon as λ_- is sufficiently smaller than λ_+, as is the case here.

We have calculated B_{c2} numerically for the material parameters above, optimizing the parameter τ such that B_{c2} is maximized. In Fig. 2 we show our result for the anisotropy ratio $\Gamma = B_{c2}^{ab}/B_{c2}^{c}$ as a function of temperature for different values of the interband coupling strength η. For $\eta = 0$, when there is no coupling between the two bands, the temperature dependence of Γ is determined by the cylindrical σ band because of its stronger pairing interaction. Here, Γ changes only by 20%, as one expects for an isotropic single gap superconductor. When η is increased, however, the temperature dependence of Γ becomes more pronounced. Our result for the parameters given above is shown as the dashed line. Note that our calculation is parameter-free, relying only on the parameters given by band structure calculations. For comparison, also the experimental data by Lyard *et al.* [20] are shown (solid circles). As will become clear below, the most important parameters determining the temperature dependence of Γ are the interband coupling strength η and the c-axis dispersion parameter ϵ_c. If we allow these two parameters to vary somewhat, we can obtain an excellent fit of the experimental data. The dotted line shows our result for $\eta = 0.121$ and $\epsilon_c = 0.182$, where the other parameters have been kept constant. We mention here that this set of parameters also gives a correspondingly good fit of the temperature dependences of B_{c2}^{c} and B_{c2}^{ab}, separately including the upward curvature of B_{c2}^{ab} that has been noted in the experiments [29]. This is just an immediate consequence of the strong temperature dependence of the anisotropy ratio and B_{c2}^{c} varying linearly near T_c because of an absence of vortex lattice distortion in this field direction.

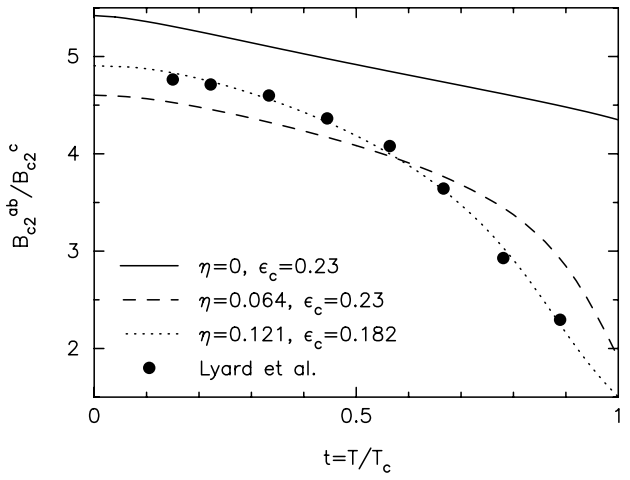

FIG. 2. Temperature dependence of the anisotropy ratio $\Gamma = B_{c2}^{ab}/B_{c2}^{c}$ for the two-band model described in the text and different interband coupling strengths η. Solid circles are experimental results taken from Lyard *et al.* [20].

Apparently, the anisotropy ratio Γ turns out to be more sensitive to interband coupling η close to T_c than at $T = 0$. In order to get a better physical understanding for this behavior, we want to discuss some limits, in which analytical solutions for B_{c2} can be obtained. At first we consider the limit $T \to T_c$. In this case Eqs. (3) and (4) can be solved exactly, and we obtain for the angular dependence of B_{c2} as a function of the angle β the magnetic field makes with the c axis:

$$\frac{B_{c2}(\beta)}{B_{c2}(\beta = 0)} = (\cos^2\beta + A\sin^2\beta)^{-1/2}, \tag{5}$$

where $A = 2\frac{(1-\eta)\langle v_{c,\sigma}^2\rangle_\sigma + \eta\langle v_{c,\pi}^2\rangle_\pi}{(1-\eta)\langle v_{ab,\sigma}^2\rangle_\sigma + \eta\langle v_{ab,\pi}^2\rangle_\pi}$. Here, $\langle v_{c,\alpha}^2\rangle_\alpha$ is the average of the squared c-axis component of the Fermi velocity over Fermi surface α, while $\langle v_{ab,\alpha}^2\rangle_\alpha$ is the corresponding in-plane quantity. The distortion parameter τ is given by $e^{-2\tau} = \frac{B_{c2}(\beta)}{B_{c2}(\beta=0)}$. When we introduce the numerical values for $v_{F\pi}$, $v_{F\sigma}$, and κ given above, we find for the anisotropy ratio

$$\frac{B_{c2}^{ab}}{B_{c2}^{c}} = \frac{1}{\sqrt{A}} = \frac{1}{\epsilon_c}\sqrt{\frac{1 + 0.63\eta}{1 + \eta(\frac{3.69}{\epsilon_c^2} - 1)}}. \tag{6}$$

For $\epsilon_c = 0.23$ this result is shown in Fig. 3 as a function of η (solid line). From Eq. (6) we see that at $\eta = 0$ the anisotropy is given by the c-axis dispersion of the cylindrical Fermi surface and actually diverges for $\epsilon_c \to 0$. (Note that this divergence could not have been obtained from a Landau level expansion above the Abrikosov ground state and our variational ansatz above is crucial for this result). Once the interband coupling η is increased, the anisotropy quickly reduces. This reduction becomes sizable already, when $\eta \sim \frac{\langle v_{c,\sigma}^2\rangle_\sigma}{\langle v_{c,\pi}^2\rangle_\pi} = \frac{\epsilon_c^2}{3.69}$. Thus, it

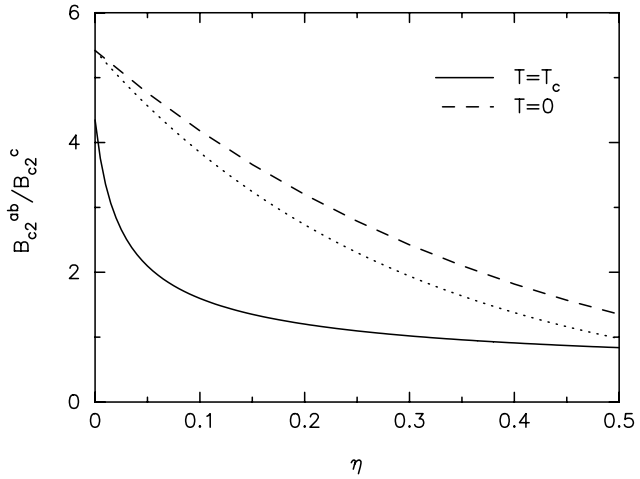

FIG. 3. Anisotropy ratio $\Gamma = B_{c2}^{ab}/B_{c2}^{c}$ as a function of interband coupling strength η for $T = 0$ (dashed line) and $T = T_c$ (solid line). The dotted line shows the approximation for $T = 0$ given in Eq. (7). At T_c the anisotropy ratio is much more sensitive to small interband coupling strengths η.

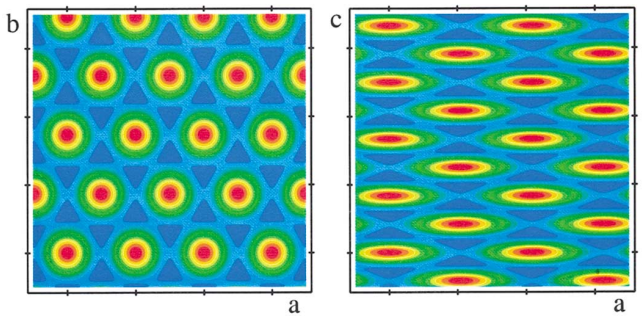

FIG. 4 (color). Vortex lattice structure for magnetic field in c-axis direction (left panel) and in ab-plane direction (right panel) at zero temperature near B_{c2} calculated from the two-band model described in the text. For comparison, the area of the unit cell has been kept fixed.

is the small c-axis Fermi velocity of the cylindrical Fermi surface as compared to the one of the π band which leads to a high sensitivity of Γ near T_c, and a small interband coupling is already sufficient to make the influence of the π band visible. In the limit $T \to 0$ the integration in Eq. (4) can be performed, and we find $l_\alpha(\tau, \frac{B_{c2}}{T^2}) = \frac{1}{2}\ln(\frac{\gamma e B_{c2}}{2\pi^2 T^2}) + \frac{1}{2}\langle \ln(e^{-2\tau} v_{F1,\alpha}^2 + e^{2\tau} v_{F2,\alpha}^2)\rangle_\alpha$ where $\ln\gamma = 0.577$. Since the pairing interaction is dominant in the σ band, we can employ two approximations: at first we set $\lambda_- = 0$. This corresponds to assuming that superconductivity in the π band is completely induced by interband coupling. As a second approximation we assume that the vortex lattice distortion τ is also dominated by the σ band. Then we can find τ by just optimizing it at $\eta = 0$ and then use it for evaluation at $\eta > 0$. With these two approximations the logarithmic averages in l_α can be performed and we finally get

$$\frac{B_{c2}^{ab}(T=0)}{B_{c2}^{c}(T=0)} = \frac{1.246}{\epsilon_c} e^{-\eta(0.482 - 2\ln\epsilon_c)}. \qquad (7)$$

The parameter τ is found to be $\tau = \frac{1}{2}\ln\epsilon_c$, which shows that at low temperatures there is no simple relation anymore between τ and the anisotropy ratio. Also we mention here that at low temperatures Eq. (5) does not hold anymore. In Fig. 3 Eq. (7) is shown for $\epsilon_c = 0.23$ as the dotted line. In order to demonstrate the quality of these approximations also the fully numerical result without these approximations is shown as the dashed line. Apparently, now the anisotropy Γ is much less sensitive to interband coupling and varies only on a scale given by $\eta \sim 1/(0.482 - 2\ln\epsilon_c)$, since ϵ_c now comes in only logarithmically. Equation (7) shows that at $T = 0$ the divergence for $\epsilon_c \to 0$ appears at all $\eta < 0.5$, while at $T = T_c$ this divergence shows up only at $\eta = 0$. Numerically we observe that at finite η and $\epsilon_c = 0$ there is a certain temperature at which B_{c2}^{ab} diverges. This temperature becomes smaller when η is increased. In Fig. 4 we show the distortion of the vortex lattice at high magnetic field and low temperature that we expect from our calculation. When the magnetic field is directed along the c axis of the crystal a regular Abrikosov lattice is expected as shown in Fig. 4 (left panel). However, when the field is directed within the ab plane we expect a distortion of $e^\tau = \sqrt{\epsilon_c} = 0.48$ as shown in Fig. 4 (right panel). This prediction can be checked by neutron scattering or STM tunneling [30].

To summarize, we have calculated the anisotropy of the upper critical field for the two band Fermi surface topology shown in Fig. 1. Using parameters from band structure calculations for MgB_2 we find a strong temperature dependence of the upper critical field in agreement with recent measurements on MgB_2 single crystals. Fine tuning of the parameters can yield a very good fit of the experimental data. We observe that the small c-axis dispersion of the σ-band leads to a high sensitivity of the anisotropy ratio on the interband coupling strength near T_c, but not at $T = 0$. This suggests that the interplay of these two quantities leads to the strong temperature dependence of the upper critical field in MgB_2.

[1] J. Nagamatsu *et al.*, Nature (London) **410**, 63 (2001).
[2] Y. Kong *et al.*, Phys. Rev. B **64**, 020501(R) (2001).
[3] A. Y. Liu, I. I. Mazin, and J. Kortus, Phys. Rev. Lett. **87**, 087005 (2001).
[4] K.-P. Bohnen *et al.*, Phys. Rev. Lett. **86**, 5771 (2001).
[5] F. Manzano *et al.*, Phys. Rev. Lett. **88**, 047002 (2002).
[6] H. D. Yang *et al.*, Phys. Rev. Lett. **87**, 167003 (2001).
[7] P. Szabo *et al.*, Phys. Rev. Lett. **87**, 137005 (2001).
[8] F. Giubileo *et al.*, Phys. Rev. Lett. **87**, 177008 (2001).
[9] F. Bouquet *et al.*, Europhys. Lett. **56**, 856 (2001).
[10] A. V. Sologubenko *et al.*, Phys. Rev. B **66**, 014504 (2002).
[11] F. Bouquet *et al.*, Phys. Rev. Lett. **89**, 257001 (2002).
[12] M. Iavarone *et al.*, Phys. Rev. Lett. **89**, 187002 (2002).
[13] S. V. Shulga *et al.*, cond-mat/0103154.
[14] J. Kortus *et al.*, Phys. Rev. Lett. **86**, 4656 (2001).
[15] A. Carrington *et al.*, cond-mat/0304435.
[16] H. J. Choi *et al.*, Nature (London) **418**, 758 (2002).
[17] I. I. Mazin *et al.*, Phys. Rev. Lett. **89**, 107002 (2002).
[18] M. Angst *et al.*, Phys. Rev. Lett. **88**, 167004 (2002).
[19] Yu. Eltsev *et al.*, Phys. Rev. B **65**, 140501(R) (2002).
[20] L. Lyard *et al.*, Phys. Rev. B **66**, 180502(R) (2002).
[21] A. I. Posazhennikova, T. Dahm, and K. Maki, Europhys. Lett. **60**, 134 (2002).
[22] B. B. Jin *et al.*, Phys. Rev. B **66**, 104521 (2002).
[23] T. Dahm *et al.*, Acta Phys. Pol. B **34**, 549 (2003).
[24] For a review see C. T. Rieck, K. Scharnberg, and N. Schopohl, J. Low Temp. Phys. **84**, 381 (1991).
[25] N. Schopohl, J. Low Temp. Phys. **41**, 409 (1980).
[26] T. Dahm, S. Graser, C. Iniotakis, and N. Schopohl, Phys. Rev. B **66**, 144515 (2002).
[27] Y. Sun and K. Maki, Phys. Rev. B **47**, 9108 (1993).
[28] A. Brinkman *et al.*, Phys. Rev. B **65**, 180517(R) (2002).
[29] T. Dahm *et al.*, cond-mat/0304194.
[30] M. R. Eskildsen *et al.*, Phys. Rev. Lett. **89**, 187003 (2002).